segregation (and possibly identification of speakers) on the basis of spatial cues (*31*, *32*).

The usefulness of natural complex sounds as stimuli in higher auditory areas has been emphasized previously (*4*, *13*). The selectivity for specific types of MCs, as found in auditory belt neurons, is higher than expected. However, even in AL, neurons rarely responded to a single call [although they sometimes responded to calls within the same phonetic category (*33*)]. This suggests that AL is still far from the end-stage in processing auditory objects, and recordings from awake animals in even more anterior and lateral areas of the STG may be promising. On the other hand, lack of extreme selectivity may also indicate that complex auditory patterns, such as vocalizations, are coded by networks of neurons rather than a single cell.

References and Notes

1. M. Konishi, T. T. Takahashi, H. Wagner, W. E. Sullivan, C. E. Carr, in *Auditory Function. Neurobiological Bases of Hearing*, G. M. Edelman, W. E. Gall, W. M. Cowan, Eds. (Wiley, New York, 1988), pp. 721–745.
2. W. M. Jenkins, M. M. Merzenich, *J. Neurophysiol.* **52**, 819 (1984).
3. H. E. Heffner, R. S. Heffner, *J. Neurophysiol.* **64**, 915 (1990).
4. J. P. Rauschecker, B. Tian, M. Hauser, *Science* **268**, 111 (1995).
5. J. H. Kaas, T. A. Hackett, M. J. Tramo, *Curr. Opin. Neurobiol.* **9**, 164 (1999).
6. L. G. Ungerleider, M. Mishkin, in *Analysis of Visual Behaviour*, D. J. Ingle, M. A. Goodale, R. J. W. Mansfield, Eds. (MIT Press, Cambridge, MA, 1982), pp. 549–586.
7. D. N. Pandya, E. H. Yeterian, in *Cerebral Cortex*, A. Peters, E. G. Jones, Eds. (Plenum, New York, 1985), vol. 4, pp. 3–61.
8. A. Morel, P. E. Garraghty, J. H. Kaas, *J. Comp. Neurol.* **335**, 437 (1993).
9. E. G. Jones, E. Dell'Anna, M. Molinari, E. Rausell, T. Hashikawa, *J. Comp. Neurol.* **362**, 153 (1995).
10. T. A. Hackett, I. Stepniewska, J. H. Kaas, *J. Comp. Neurol.* **394**, 475 (1998).
11. L. M. Romanski *et al.*, *Nature Neurosci.* **2**, 1131 (1999).
12. T. A. Hackett, I. Stepniewska, J. H. Kaas, *J. Comp. Neurol.* **400**, 271 (1998).
13. J. P. Rauschecker, *Curr. Opin. Neurobiol.* **8**, 516 (1998).
14. J. P. Rauschecker, B. Tian, T. Pons, M. Mishkin, *J. Comp. Neurol.* **382**, 89 (1997).
15. G. H. Recanzone, D. C. Guard, M. L. Phan, T. K. Su, *J. Neurophysiol.* **83**, 2723 (2000).
16. A total of 80 penetrations perpendicular to the open surface of the STG were made with lacquer-coated tungsten electrodes along the lateral sulcus of four rhesus monkeys (*Macaca mulatta*), lightly anesthetized with isoflurane (0.5 to 1.5%) and nitrous oxide (50%). All studies were performed within a double-walled sound-proof chamber (3.05 m by 2.85 m by 1.98 m) whose inside walls were covered with 4-inch-thick acoustic foam to minimize standing waves and echoes. Single units were isolated with the aid of a window discriminator and a slicer unit (*34*). BF_c of each unit was determined with BPN stimuli presented through the center speaker. The borders between two adjacent belt areas were identified from the reversal point of the BF_c. BPN stimuli were 200 ms long with a rise-and-fall time of 5 ms. All sounds were energy-matched on the basis of root-mean-square values and were played at sound pressure levels of 45 to 75 dB, i.e., well in the suprathreshold range. When several levels were tested, the best response was used for analysis.
17. Digitized calls recorded from free-ranging monkeys were used for stimulation. The calls can be subdivided phonetically into three major groups: tonal, harmonic, and noisy calls (*35*).
18. Each of the seven MCs was played back in succession at all seven positions, from the most contra- to the most ipsilateral, and this was repeated 10 times for each call. MC types were presented in a fixed order, harmonic or tonal calls alternating with noisy calls (see Fig. 1B and the vertical scale of Fig. 2). An alternative design, in which positions and MCs were completely randomized, was abandoned in favor of the standardized sequence, because it poses the risk of total data loss when a neuron is lost prematurely. A comparison of the results from random and standardized stimulus presentation in several neurons did not reveal any significant differences, and stability of recordings was always monitored from raster displays. Only complete data sets from a total of 251 units were used. The spikes in response to stimulation were added up into 49 MC- and position-specific peristimulus time histograms (PSTHs). All PSTHs had a prestimulus interval of 500 ms, from which baseline activity was determined. Net responses were quantified from averaged peak firing rates with a 40-ms "sliding window" and normalized. The MC that elicited the maximal response was defined as the preferred monkey call, and the spatial position of that call as the preferred azimuth. An MCPI was defined as the number of MCs to which a neuron yielded a response >50% of the maximum at the preferred azimuth. Spatial selectivity was determined by the width of the half-maximal response to the preferred monkey call across azimuth. Neurons were considered spatially tuned if their response fell to less than 50% of the maximum at any other spatial position and were classified as "contra-field," "ipsi-field," or "single-peak" (*36*). Of all preferred azimuths, 59% fell into the contralateral, 32% into the ipsilateral hemifield, and 9% were straight ahead (0°). This distribution was similar in all three belt areas ($P > 0.1$, χ^2-test).
19. One of the monkeys was prepared for semichronic recording (*37*), so that both CL and AL could be mapped exhaustively in repeated sessions. A recording chamber and head bolt were mounted on the animal's skull in a single aseptic surgery under gas anesthesia. Fifteen recording sessions, each lasting 6 to 8 hours, were subsequently performed under the same conditions as in the acute experiments.
20. When measured with BPN bursts, spatial half-width was very similar ($n = 38$; $P > 0.05$, Wilcoxon signed rank test for pairwise comparisons) (*33*), and the difference between AL and CL, despite the small sample size, was still significant ($P < 0.05$, Mann-Whitney U test).
21. J. P. Rauschecker, B. Tian, *Proc. Natl. Acad. Sci. U.S.A.* **97**, 11800 (2000).
22. K. O. Bushara *et al.*, *Nature Neurosci.* **2**, 759 (1999).
23. T. D. Griffiths *et al.*, *Nature Neurosci.* **1**, 74 (1998).
24. J. W. Lewis, D. C. Van Essen, *J. Comp. Neurol.* **428**, 112 (2000).
25. L. Leinonen, J. Hyvärinen, A. R. A. Sovijärvi, *Exp. Brain Res.* **39**, 203 (1980).
26. M. S. A. Graziano, L. A. J. Reiss, C. G. Gross, *Nature* **397**, 428 (1999).
27. T. A. Hackett, I. Stepniewska, J. H. Kaas, *Brain Res.* **817**, 45 (1999).
28. J. R. Binder *et al.*, *Cereb. Cortex* **10**, 512 (2000).
29. P. Belin, R. J. Zatorre, P. Lafaille, P. Ahad, B. Pike, *Nature* **403**, 309 (2000).
30. S. K. Scott, C. C. Blank, S. Rosen, R. J. S. Wise, *Brain* **123**, 2400 (2000).
31. D. E. Broadbent, *Perception and Communication* (Pergamon, London, 1958).
32. A. S. Bregman, *Auditory Scene Analysis* (MIT Press, Cambridge, MA, 1990).
33. Supplementary data are available on *Science* Online at www.sciencemag.org/cgi/content/full/292/5515/290/DC1.
34. B. Tian, J. P. Rauschecker, *J. Neurophysiol.* **79**, 2629 (1998).
35. M. D. Hauser, *The Evolution of Communication* (MIT Press, Cambridge, MA, 1996).
36. R. Rajan, L. M. Aitkin, D. R. F. Irvine, J. McKay, *J. Neurophysiol.* **64**, 872 (1990).
37. J. P. Rauschecker, M. Korte, *J. Neurosci.* **13**, 4538 (1993).

38. The help of A. Lord, E. MacStravic, and C. Silver with recording and animal care is acknowledged gratefully. M. Hauser provided the monkey calls. Supported by U.S. Department of Defense (grant DAMD17-93-V-3018) and NIH (grants R01-DC03489 and R03-DC03845 to J.P.R. and B.T., respectively).

10 January 2001; accepted 8 March 2001

G Protein βγ Subunit–Mediated Presynaptic Inhibition: Regulation of Exocytotic Fusion Downstream of Ca^{2+} Entry

Trillium Blackmer,[1,3] Eric C. Larsen,[5] Michiko Takahashi,[2] Thomas F. J. Martin,[5] Simon Alford,[2,4]* Heidi E. Hamm[1,3]*†

The nervous system can modulate neurotransmitter release by neurotransmitter activation of heterotrimeric GTP–binding protein (G protein)–coupled receptors. We found that microinjection of G protein βγ subunits (Gβγ) mimics serotonin's inhibitory effect on neurotransmission. Release of free Gβγ was critical for this effect because a Gβγ scavenger blocked serotonin's effect. Gβγ had no effect on fast, action potential–evoked intracellular Ca^{2+} release that triggered neurotransmission. Inhibition of neurotransmitter release by serotonin was still seen after blockade of all classical Gβγ effector pathways. Thus, Gβγ blocked neurotransmitter release downstream of Ca^{2+} entry and may directly target the exocytotic fusion machinery at the presynaptic terminal.

A number of neurotransmitters have been shown to modulate release from presynaptic terminals (*1, 2*) through activation of a G protein–coupled receptor (GPCR) (*3, 4*). The two arms of activated G proteins, Gα and Gβγ, may exert their modulatory effect by

regulating second messenger enzymes, ion channels, or other targets (*5*). The cellular and molecular mechanisms underlying GPCR-mediated presynaptic modulation remain largely undetermined because of the difficulties in manipulating and recording from presynaptic terminals. The reticulospinal/motoneuron synapse in the lamprey is one of the few vertebrate synapses that are experimentally accessible both pre- and postsynaptically, because of their large size. In this giant synapse, serotonin decreases the efficacy of synaptic transmission presynaptically (*6, 7*) through a GPCR.

We microinjected proteins into the presynaptic terminal and determined the effect of serotonin on the strength of synaptic transmission. We recorded from pre-and postsynaptic elements simultaneously (*6, 8*), as indicated in Fig. 1A. Presynaptic axons were stimulated intracellularly to evoke excitatory postsynaptic currents (EPSCs) in the postsynaptic neurons. This resulted in mixed electrical and chemical EPSCs (Fig. 1B, part ii). Separation between the two components was clear with a fast invariable electrical component and a slower chemical component that exhibited quantal variation in amplitude (Fig. 1C, part i). The averaged postsynaptic responses before and after exposure to serotonin (30 μM) are shown in Fig. 1B, part ii. Application of serotonin reduced the amplitude of the chemical component to 19.8 ± 7.5% of the control's amplitude [four pairs; $P < 0.01$ (*9*)] (Fig. 1B, part ii). Serotonin-mediated depression was seen concurrently with application of serotonin (<1 min) without affecting the amplitude of the electrical component. This serotonin-mediated depression of synaptic transmission is presynaptic (*6*) and is independent of the modulation of Ca^{2+} entry into the presynaptic terminal (*7*).

Serotonin works via a GPCR in this synapse. After activation by a GPCR, the G protein dissociates into an activated GαGTP subunit (GTP, guanosine 5′-triphosphate) and a free Gβγ subunit (*10*). Which G protein subunit inhibits neurotransmitter release is not known. We thus injected proteins directly into the presynaptic terminal (*11*). Injection of vehicle had no significant effect ($n = 3$; EPSC amplitude changed to 104 ± 7% of the control's amplitude) on the EPSCs evoked in paired-cell recording (Fig. 1D). We injected $G\beta_1\gamma_2$ directly into the intracellular space of the presynaptic terminal through the microelectrode while simultaneously recording from the postsynaptic neuron. We chose the

[1]Department of Molecular Pharmacology and Biological Chemistry, [2]Department of Physiology, [3]Northwestern University Institute for Neuroscience, Northwestern University Medical School, 303 East Chicago Avenue, Chicago, IL 60611, USA. [4]Department of Biological Sciences, University of Illinois at Chicago, 840 West Taylor Street, Chicago, IL 60608, USA. [5]Department of Biochemistry, University of Wisconsin at Madison, Madison, WI 53706, USA.

*To whom correspondence should be addressed. E-mail: sta@uic.edu (S.A.) and heidi.hamm@mcmail.vanderbilt.edu (H.E.H.)

†Present address: Department of Pharmacology, 442 Robinson Research Building, Vanderbilt University Medical Center, Nashville, TN 37232, USA.

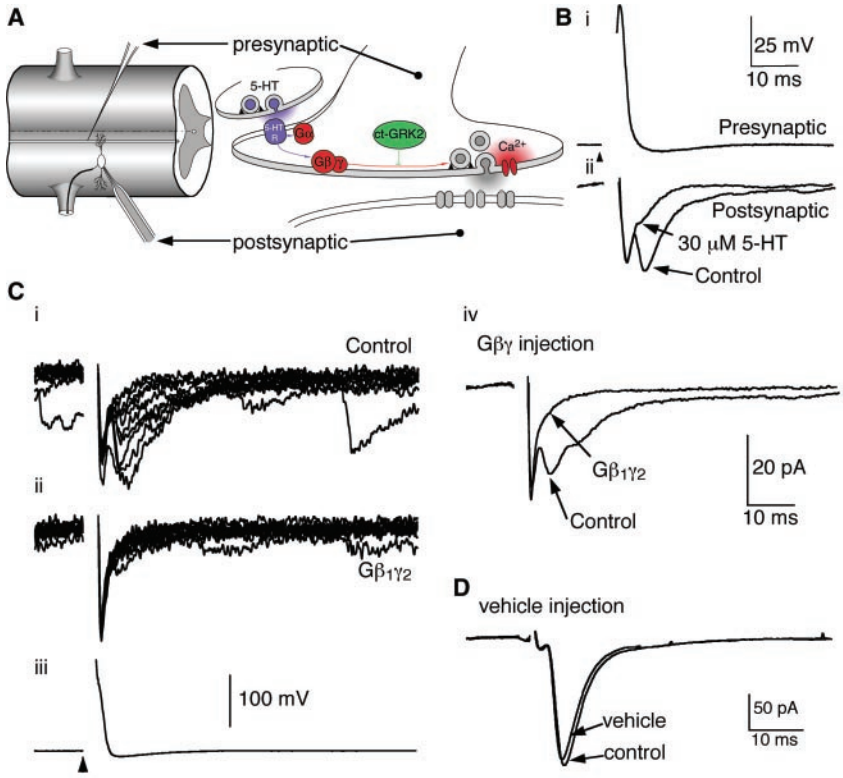

Fig. 1. Serotonin (5-HT) and presynaptic Gβγ inhibit neurotransmitter release. (**A**) (Left) Schematic diagram to show the recording arrangement in paired recordings between reticulospinal axons and ventral horn neurons. The axon is held under current clamp with a microelectrode, and the motoneuron is simultaneously held under voltage clamp with a patch electrode. 5-HT R, serotonin receptor. (Right) A hypothesized signaling cascade evoked by serotonin released onto the presynaptic cell. (**B**) Serotonin (30 μM) inhibits synaptic transmission at the giant reticulospinal synapse. Part i shows presynaptic recordings from a giant axon. The presynaptic action potential was evoked by a depolarizing current pulse (2 ms) through the recording microelectrode. Part ii shows the presynaptic action potential–evoked EPSCs in the postsynaptic motoneuron. The application of serotonin reduced the amplitude of the EPSC but had no effect on the membrane potential. These data represent the mean responses of 20 consecutive trials. (**C**) The pressure injection of $G\beta_1\gamma_2$ to the presynaptic axon had no effect on the membrane potential or evoked presynaptic action potential (part iii) but reduced the amplitude of the EPSC (part i). Part iv is the average of 20 consecutive traces; raw traces are also shown before (part i) and after (part ii) microinjection of $G\beta_1\gamma_2$. (**D**) Microinjection of the carrier vehicle has no effect on transmitter release (data are the average of 20 consecutive trials).

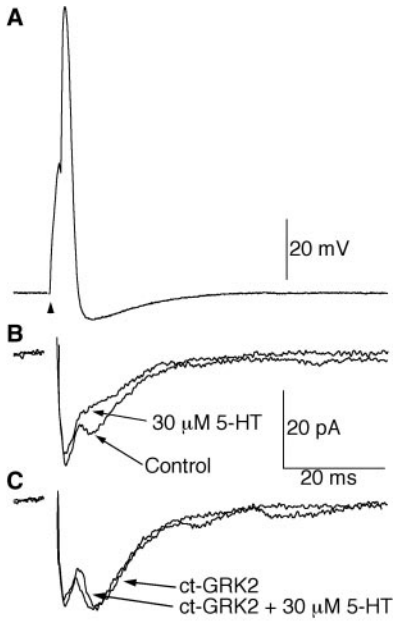

Fig. 2. A Gβγ scavenger blocks the inhibitory effect of serotonin. (**A**) The presynaptic action potential evoked a postsynaptic EPSC that was reduced by serotonin (5-HT). (**B**) Control EPSCs are the mean of 12 consecutive stimuli from a typical ventral horn neuron. The presynaptic microinjection of ct-GRK2 results in an enhancement of the EPSC amplitude over control conditions recorded over the following 30 min, although this enhancement was not significant. (**C**) ct-GRK2 attenuates inhibition of neurotransmission by serotonin application.

$G\beta_1\gamma_2$ subunit combination because it is widely distributed within the central nervous system (*12*). The averaged postsynaptic responses before and after $G\beta_1\gamma_2$ pressure injection are shown in Fig. 1C, part iv. A number of individual EPSCs before and after $G\beta_1\gamma_2$ injection are shown in Fig. 1C, parts i and ii. $G\beta_1\gamma_2$ inhibited the chemical component of neurotransmission to 35 ± 23% of that of the control ($n = 6$; $P < 0.01$) while leaving the electrical component unaltered.

Gβγ can mimic serotonin's effect on synaptic transmission, but is it normally a part of the serotonin-mediated signaling cascade? A scavenger of Gβγ, the carboxyl terminus of the G protein–coupled receptor kinase 2 (ct-GRK2), was microinjected into the presynaptic axon (*13*). ct-GRK2 is a potent and specific Gβγ inhibitor (*14*). If the inhibition of neurotransmission by activation of serotonin receptors is via Gβγ, then ct-GRK2 should attenuate this inhibition. The addition of 30 μM serotonin to the superfusate resulted in a reduction of the chemical component of the EPSC (Fig. 2B). After serotonin was washed out, ct-GRK2 was microinjected into the presynaptic axon. Reapplication of serotonin (30 μM) had no effect on the amplitude of the evoked EPSC ($n = 5$) after microinjection of ct-GRK2 (Fig. 2C). Thus, the Gβγ scavenger completely occluded the ability of serotonin to inhibit chemical neurotransmission.

We performed Ca^{2+} imaging experiments (*15*) to examine the effect of serotonin application or $G\beta_1\gamma_2$ microinjection on the fast Ca^{2+} transient elicited by presynaptic action potentials. We have previously demonstrated that high-affinity dyes [e.g., Oregon Green 488 BAPTA-1 (BAPTA, 1,2-bis(2-aminophenoxy)ethane-*N*,*N*,*N*′,*N*′-tetraacetic acid)] may be used to measure Ca^{2+} transients evoked after action potential activation of voltage-gated Ca^{2+} channels in giant axons (*16*). This allows us to examine serotonin or Gβγ modulation of voltage-gated Ca^{2+} channels or modulation of other ion channels, which could, in turn, change the gating of Ca^{2+} channels during an action potential. The amplitude of these Ca^{2+} transients can be correlated with neurotransmitter release (*7*). Single action potentials were evoked in the presynaptic axons through a stimulating electrode (Fig. 3A). An action potential–mediated Ca^{2+} transient was observed, which results from the activation of Ni^{2+}-sensitive voltage-operated Ca^{2+} channels in this preparation (*7, 15*). Serotonin (30 μM) slightly reduced the peak amplitude of this stimulus-evoked Ca^{2+} transient (the mean change was to 82.1 ± 3.9% of that of the control; $P < 0.0001$; $n = 28$) (Fig. 3B). We repeated this experiment with a low-affinity indicator

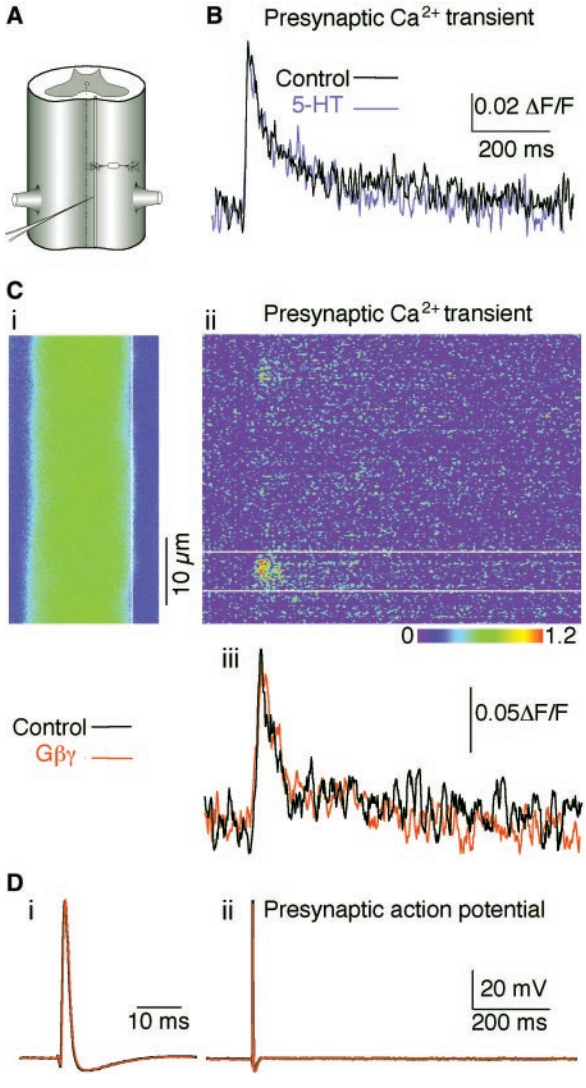

Fig. 3. $G\beta_1\gamma_2$ has no effect on stimulus-evoked presynaptic Ca^{2+} transients. (**A**) Schematic to show the recording arrangement during Ca^{2+} imaging experiments. Axons were stimulated either through a microelectrode for Gβγ injections or extracellularly for experiments with serotonin (5-HT) application. Reticulospinal axons were labeled with the calcium-sensitive dye Oregon Green 488 BAPTA-1 [an example is shown in (C)]. (**B**) A single action potential was evoked in the axon by extracellular stimulation. This evoked a transient increase in axonal Ca^{2+}, and localized areas of Ca^{2+} influx or "hot spots" are observed [e.g., part ii of (C)]. Data are normalized to prestimulus levels. The fluorescent response ($\Delta F/F$) was integrated at each time point and plotted as a function of time (black trace, control data). The application of serotonin (30 μM) showed little effect on the amplitude of the evoked Ca^{2+} transient (blue trace). (**C**) Part i shows the axon filled with Oregon Green 488 BAPTA-1. Image data were taken from repeated scanning from the vertical white line at 500 Hz. The data were recorded from this axon with a microelectrode containing $G\beta_1\gamma_2$. In part ii, the transient increase in fluorescence is seen in response to an action potential evoked by intracellular current injection. Part iii shows the signal integrated from part ii before (black) and 30 min after (red) the intracellular injection of Gβγ. Data are shown with the same time scale as in part ii of both (C) and (D). (**D**) As seen in part i, microinjection of $G\beta_1\gamma_2$ had no effect on stimulus-evoked action potentials [the axon shown in (C), parts i and ii]. The action potential is shown before (black) and 30 min after (red) the injection of Gβγ into the presynaptic axon. Part ii shows the same data but on a time scale compressed to that of the image [(C), part ii]. The axon was stimulated intracellularly to evoke an action potential.

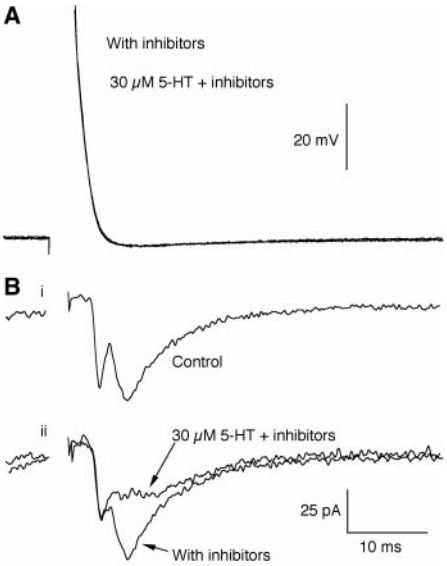

Fig. 4. Blockade of kinases and phosphatases does not prevent the inhibition of neurotransmission by serotonin (5-HT). Paired recordings between a reticulospinal axon and a motoneuron are shown. (**A**) Presynaptic stimulation evoked an action potential. This was not altered by the application of free phosphate to block phosphatases (200 mM KPO_4^-) through the presynaptic recording electrode and the application of 1 μM wortmannin, 10 μM genistein, and 10 μM staurosporin to the superfusate to block PI 3-kinase, tyrosine kinases, and Ser/Thr kinases, respectively (control not shown). Subsequent addition of serotonin also did not alter the action potential. (**B**) The presynaptic action potential results in a postsynaptic EPSC with an electrical and chemical component. The application of phosphatase and kinase inhibitors neither altered the response (parts i and ii) nor prevented serotonin-mediated inhibition of neurotransmitter release (part ii). Data are the mean of 10 consecutive trials.

[Fluo-4 dextran (dissociation constant $K_d \cong 3$ μM)] (*17*). A similar lack of effect of serotonin on the amplitude of the Ca^{2+} transient was observed (amplitude after serotonin application was 95% of the control's amplitude; $n = 2$) (*18*). Furthermore, serotonin has no effect on Ca^{2+} currents recorded from giant axons under whole-cell voltage-clamp conditions (*7*). The reduction in peak amplitude of the Ca^{2+} transient cannot account for the profound depression of the EPSCs elicited by application of serotonin.

GPCRs modulate voltage-gated Ca^{2+} channels in the soma of cultured lamprey dorsal cells (*19*), as in other preparations (*20–25*). We thus performed Ca^{2+} imaging experiments as described above. Control Ca^{2+} transients were recorded (Fig. 3C, parts ii and iii), and then the presynaptic axons were loaded with $G\beta_1\gamma_2$. Microinjected $G\beta_1\gamma_2$ had no significant effect on evoked Ca^{2+} transients (mean change in Ca^{2+} transient amplitude was to 99.6 ± 0.25% of the control's amplitude after injection of $G\beta_1\gamma_2$; $P < 0.01$; $n = 6$) (Fig. 3C, part iii). Similarly, $G\beta_1\gamma_2$ injection had no effect on the amplitude or duration of the presynaptic action potential (Fig. 3D, parts i and ii). Therefore, presynaptic Gβγ does not control evoked Ca^{2+} entry through voltage-gated Ca^{2+} channels and must mediate its inhibitory effect on neurotransmitter release downstream of Ca^{2+} entry.

There are many known Gβγ effectors, including adenylyl cyclase II (AC II), phosphatidylinositol 3-kinase (PI 3-kinase), phospholipase C–β2 (PLC-β2), and several tyrosine kinases (*5*). Any of these effectors could mediate the inhibition of neurotransmitter release. We wanted to block all known Gβγ effectors, as well as any possible Gβγ regulation of Ser/Thr kinases or phosphatases, and determine whether serotonin inhibition of synaptic transmission could still occur. Application of forskolin has no effect on the serotonin-mediated inhibition of the EPSC (*7*). Therefore, it is unlikely that Gβγ works via AC II. We have shown that Gβγ does not cause a change in the internal Ca^{2+} concentration (*7*); thus, PLC-β2 is not a likely target. Presynaptic phosphatases were blocked by injection of 200 mM free phosphate through the presynaptic recording pipette. Gβγ activation of PI 3-kinase was blocked by wortmannin (1 μM), activation of tyrosine kinases was blocked by the wide-spectrum tyrosine kinase inhibitor genistein (10 μM), and activation of Ser/Thr kinases was blocked by staurosporine (1 μM). This cocktail of inhibitors did not occlude the ability of serotonin to inhibit neurotransmission ($n = 4$; serotonin reduced the evoked response to 23.5 ± 12% of that of the control) (Fig. 4B). These data suggest that Gβγ inhibition of neurotransmitter release is not mediated via classical Gβγ effectors or via other unknown effectors that may involve Ser/Thr or Tyr kinases or phosphatases. Thus, we considered the possibility that Gβγ may act directly on the exocytotic machinery that mediates vesicle fusion.

We conducted binding assays with purified $G\beta_1\gamma_2$ and glutathione *S*-transferase (GST) fusion proteins syntaxin1A (amino acids 1 through 265), soluble *N*-ethylmaleimide–sensitive factor attachment protein (SNAP)–25B, and vesicle-associated membrane protein (VAMP) II (amino acids 1 through 94) (*26*). $G\beta_1\gamma_2$ binding to syntaxin (*27*) and SNAP-25 was detected while binding to ternary soluble *N*-ethylmaleimide–sensitive factor attachment protein receptor (SNARE) complexes consisting of syntaxin, SNAP-25, and VAMP was markedly enhanced in comparison to either syntaxin or SNAP-25 binding alone.

Various GPCRs and G proteins modulate synaptic neurotransmitter secretion at several sites either upstream from, at, or downstream from Ca^{2+} entry mechanisms. In neuronal cell bodies, in transfected cell lines, and in *Xenopus* oocytes (*28–31*), Gβγ directly activates a class of G protein–coupled inwardly rectifying K^+ channels that would result in inhibited Ca^{2+} entry. GPCR-mediated inhibition of neurotransmitter release via inhibition of voltage-gated Ca^{2+} channels has also been demonstrated at one presynaptic terminal (*32, 33*). The ability of G proteins to mediate inhibition of synaptic neurotransmitter release at a step beyond Ca^{2+} entry was first demonstrated in the neuromuscular junction (*34, 35*). Spontaneous exocytotic events can be detected by recording miniature postsynaptic currents (mPSCs). mPSCs are modulated by many GPCRs (*7, 36, 37*). Biochemical studies also support the idea that G protein activation inhibits neurotransmitter or hormone release downstream from Ca^{2+} entry, because the inhibitory effects of GPCR activation are preserved after cell permeabilization (*38*).

Our results show that Gβγ, and not Gα, is the active G protein subunit that mediates the Ca^{2+}-independent pathway of a GPCR's presynaptic inhibition. We demonstrated that Gβγ inhibits neurotransmitter release downstream of Ca^{2+} entry mechanisms. By blocking endogenous Gβγ activity, we also showed that activation of a GPCR requires free Gβγ to inhibit neurotransmitter release, because a Gβγ scavenger blocked the serotonin inhibition. Moreover, the serotonin inhibition persisted in the presence of agents that block classical Gβγ effector pathways, indicating that Gβγ may affect transmitter release mechanisms directly. Gβγ binds SNARE proteins syntaxin (*27*), SNAP-25, and the ternary SNARE complex, suggesting that Gβγ could directly target the fusion machinery to inhibit vesicular release. The mechanism underlying GPCR-mediated presynaptic inhibition at a site distal to Ca^{2+} entry may involve a direct interaction between Gβγ and the core fusion machinery.

References and Notes

1. J. C. Eccles, R. F. Schmidt, W. D. Willis, *J. Neurophysiol.* **26**, 506 (1963).
2. R. A. Nicoll, B. E. Alger, *Int. Rev. Neurobiol.* **21**, 217 (1979).
3. S. Alford, S. Grillner, *J. Neurosci.* **11**, 3718 (1991).
4. R. J. Miller, *Annu. Rev. Pharmacol. Toxicol.* **38**, 201 (1998).
5. H. E. Hamm, *J. Biol. Chem.* **273**, 669 (1998).
6. J. T. Buchanan, S. Grillner, *Neurosci. Lett.* **122**, 71 (1991).
7. M. Takahashi, R. Freed, T. Blackmer, S. Alford, *J. Physiol. (London)* **532**, 323 (2001).
8. Spinal cord preparations from lamprey ammocoetes (*Petromyzon marinus*) were performed as previously described [W. O. Wickelgren, *J. Physiol. (London)* **270**, 89 (1977)]. Whole-cell patch-clamp recordings were achieved with the blind technique [M. G. Blanton, J. J. Lo Turco, A. R. Kriegstein, *J. Neurosci. Methods* **30**, 203 (1989)] by using pipettes pulled to a tip resistance of 5 to 10 megohms, as previously described (*16*). All paired recordings to measure the effect of a protein or peptide injection in this study were made at a minimum of 30 min after injection and less than 100 mm from the presynaptic injection site. Significance was determined using Student's paired *t* test. *P* values greater than 0.05 were determined to be not significant.
9. To isolate the chemical component from the partially overlapping electrical component, we measured the peak amplitude of the chemical component and subtracted it from a single exponential curve fitted to the electrical component.
10. L. Stryer, H. R. Bourne, *Annu. Rev. Cell Biol.* **2**, 391 (1986).
11. Bovine-derived recombinant $G\beta_1\gamma_2$ [C. E. Ford *et al.*, *Science* **280**, 1271 (1998)] was stored at –20°C in an internal patch solution containing 102.5 mM $MeSO_4$ (methane sulfonate), 1 mM NaCl, 1 mM $MgCl_2$, 5 mM Hepes, 0.05 mM EGTA, and 0.0025% CHAPS, which was brought to a pH of 7.4 with KOH. Concentrations ranged from 3 to 5 mg/ml. For microinjection into the presynaptic terminal, 50% by volume of 3 M $KMeSO_4$ was added to the $G\beta_1\gamma_2$-containing solution.
12. M. Betty, S. W. Harnish, K. J. Rhodes, M. I. Cockett, *Neuroscience* **85**, 475 (1998).
13. ct-GRK2 (β adrenergic receptor kinase) is composed of residues 548 through 671 of the rat homolog GRK2. ct-GRK2 (8 mg/ml) was stored at –20°C in a solution containing 20 mM acetate, 10% glycerol, 0.1% β-mercaptoethanol, 1 mM EDTA, and 0.1 mM phenylmethylsulfonyl fluoride, at pH 5.5. For microinjection into the presynaptic terminal, 50% by volume 3 M KMeSO4 or KCl was added.
14. W. J. Koch, B. E. Hawes, J. Inglese, L. M. Luttrell, R. J. Lefkowitz, *J. Biol. Chem.* **269**, 6193 (1994).
15. Imaging experiments were performed on a confocal microscope (Bio-Rad MRC600) as previously described (*16*). For Ca^{2+} imaging experiments, axons were retrogradely labeled with dextran-conjugated Oregon Green 488 BAPTA-1. Rapid Ca^{2+} transients were measured by repetitively scanning the image at a single line (500 Hz). The ability to load protein into axons by pressure ejection from the microelectrode was tested by pressure ejection of fluorescein-labeled ovalbumin. This demonstrated a near instantaneous increase in fluorescence at the recording site (the mean intensity of fluorescence was of 150 bits with a background noise measured as standard deviation of 19 bits). The ovalbumin then diffused from this injection site such that mean fluorescence in three axons was 82% of the intensity of the injection site after 30 min of recording at a distance of 100 μm from that site.
16. A. J. Cochilla, S. Alford, *Neuron* **20**, 1007 (1998).
17. A. C. Kreitzer, K. R. Gee, E. A. Archer, W. G. Regehr, *Neuron* **27**, 25 (2000).
18. Supplemental data are available at www.sciencemag.org/cgi/content/full/292/5515/293/DC1.

19. A. El Manira, W. Zhang, E. Svensson, N. Bussieres, *J. Neurosci.* **17**, 1786 (1997).
20. G. G. Holz, R. M. Kream, A. Spiegel, K. Dunlap, *J. Neurosci.* **9**, 657 (1989).
21. A. C. Dolphin *et al.*, *Biochem. Soc. Trans.* **21**, 391 (1993).
22. S. Herlitze *et al.*, *Nature* **380**, 258 (1996).
23. S. R. Ikeda, *Nature* **380**, 255 (1996).
24. M. De Waard *et al.*, *Nature* **385**, 446 (1997).
25. N. Qin, D. Platano, R. Olcese, E. Stefani, L. Birnbaumer, *Proc. Natl. Acad. Sci. U.S.A.* **94**, 8866 (1997).
26. GST fusion proteins encoded by pGEX vectors were produced in *Escherichia coli* by standard methods. Standard conditions for binding studies employed 200-μl reactions containing 0.02 M Hepes (pH 7.2), 0.15 M KCl, 0.5% Triton X-100, 0.03% CHAPS, and 1% cold fish skin gelatin. Ternary SNARE complexes were formed by overnight incubation at 4°C of SNAP-25B, syntaxin1A, or VAMPII, each at 1 μM. Incubations were for 1 hour at 4°C, after which beads were recovered by centrifugation and washed three times in 500 μl of assay buffer before solubilization in sample buffer for SDS–polyacrylamide gel electrophoresis. Electrophoresed samples were transferred to nitrocellulose for immunoblotting with a polyclonal rabbit antibody generated against Gβ used at a dilution of 1:500. Enhanced chemiluminescence was used for detection. Horseradish peroxidase–conjugated goat anti-rabbit secondary antibodies were used at a dilution of 1:20,000.
27. S. E. Jarvis, J. M. Magga, A. M. Beedle, J. E. Braun, G. W. Zamponi, *J. Biol. Chem.* **275**, 6388 (2000).
28. E. Reuveny *et al.*, *Nature* **370**, 143 (1994).
29. C. L. Huang, P. A. Slesinger, P. J. Casey, Y. N. Jan, L. Y. Jan, *Neuron* **15**, 1133 (1995).
30. P. Kofuji, N. Davidson, H. A. Lester, *Proc. Natl. Acad. Sci. U.S.A.* **92**, 6542 (1995).
31. D. E. Logothetis, Y. Kurachi, J. Galper, E. J. Neer, D. E. Clapham, *Nature* **325**, 321 (1987).
32. T. Takahashi, I. D. Forsythe, T. Tsujimoto, M. Barnes-Davies, K. Onodera, *Science* **274**, 594 (1996).
33. R. R. Mirotznik, X. Zheng, E. F. Stanley, *J. Neurosci.* **20**, 7614 (2000).
34. E. M. Silinsky, *J. Physiol. (London)* **346**, 243 (1984).
35. _____, C. S. Solsona, *J. Physiol. (London)* **457**, 315 (1992).
36. M. Umemiya, A. J. Berger, *J. Neurophysiol.* **73**, 1192 (1995).
37. J. H. Singer, A. J. Berger, *Sleep* **19**, S146 (1996).
38. A. Luini, M. A. De Matteis, *J. Neurochem.* **54**, 30 (1990).
39. We are grateful to A. Bohm, Y. Daaka, and B. M. Willardson for their generous gifts of ct-GRK2, pGex ct-GRK5, and GST-Phosducin, respectively. We thank N. Skiba for helpful suggestions regarding preparation of ct-GRK2 and Gβγ for microinjection and E. Silinsky and E. Mugnaini for their critical reading of the manuscript. This work was funded by grants from the National Eye Institute (H.E.H.), the National Institute of Diabetes and Digestive and Kidney Diseases (T.F.J.M.), and the National Institute of Neurological Disorders and Stroke (S.A.).

5 January 2001; accepted 15 March 2001

Two Functional Channels from Primary Visual Cortex to Dorsal Visual Cortical Areas

N. Harumi Yabuta, Atomu Sawatari,* Edward M. Callaway†

Relationships between the M and P retino-geniculo-cortical visual pathways and "dorsal" visual areas were investigated by measuring the sources of local excitatory input to individual neurons in layer 4B of primary visual cortex. We found that contributions of the M and P pathways to layer 4B neurons are dependent on cell type. Spiny stellate neurons receive strong M input through layer 4Cα and no significant P input through layer 4Cβ. In contrast, pyramidal neurons in layer 4B receive strong input from both layers 4Cα and 4Cβ. These observations, along with evidence that direct input from layer 4B to area MT arises predominantly from spiny stellates, suggest that these different cell types constitute two functionally specialized subsystems.

The primate visual system is characterized by dozens of distinct cortical areas, each thought to be specialized for the functional analysis of different aspects of the visual environment (*1*–*3*). These areas can be divided into a "dorsal" stream specialized for the analysis of spatial relations and a "ventral" stream specialized for object recognition. The functional differences between these areas are believed to arise in part because of differences in contributions from parallel, functionally specialized magnocellular (M) and parvocellular (P) pathways that originate in the retina and terminate in separate layers of primary visual cortex (V1)—layers 4Cα and 4Cβ, respectively (*2*–*7*). Layer 4C neurons in turn connect to neurons in more superficial layers of V1 that provide the output to "higher" dorsal and ventral areas. Specifically, ventral stream areas receive inputs directly or indirectly from layer 2/3 of V1, whereas dorsal areas receive their input from layer 4B.

Local circuits in V1 generate two functionally and anatomically distinct channels, "blobs" and "interblobs," contributing to ventral visual areas (*2*–*7*). Thus, for the ventral stream, the relationships of M and P pathways to extrastriate areas can be inferred largely from anatomical studies of the connectivity from layer 4C to blobs versus interblobs in layer 2/3 (*8*–*10*).

In layer 4B, neurons projecting to different dorsal visual areas or modules (V2 thick stripes, V3, and MT) are spatially intermingled. Thus, anatomical observations of V1 circuitry do not clearly reveal the connectional relationships between M and P pathways and the cortical areas that receive layer 4B input (*11*, *12*). Neurons in layer 4B that project to different cortical areas are morphologically distinct. In the macaque monkey, direct input to area MT (V5) comes primarily from spiny stellate neurons (*13*), whereas areas V2 and V3 also receive input from pyramidal neurons (*14*–*16*). Thus, it is possible to study the different contributions of the M and P pathways to layer 4B–recipient visual areas by using scanning laser photostimulation to identify the sources of functional input to morphologically identified cell types in layer 4B (*11*, *17*–*20*).

We used scanning laser photostimulation and whole-cell voltage-clamp recordings in living brain slices to identify the locations of neurons providing excitatory input to layer 4B neurons in macaque monkey primary visual cortex (*21*). Excitatory postsynaptic currents (EPSCs) evoked in the recorded cell after photostimulation are indicative of direct monosynaptic connections from neurons near the stimulation site to the recorded cell. Polysynaptic responses mediated by secondary neurons far from the stimulation site are ruled out because such secondary neurons do not fire action potentials (APs) under the stimulation conditions used (*20*, *21*).

Photostimulation and intracellular recording, along with subsequent anatomical and physiological analyses (*22*), yielded complete excitatory input maps for 14 layer 4B pyramidal neurons, 4 spiny stellates, and 5 inhibitory neurons. Figure 1 illustrates excitatory input maps to two pyramidal neurons (Fig. 1, A and C), one spiny stellate neuron (Fig. 1B), and one inhibitory neuron (Fig. 1D). All four neurons received strong excitatory input from layer 4Cα. Layer 4Cβ provided strong input to the pyramidal neurons but not to the spiny stellate or inhibitory neuron. These characteristics of the excitatory input patterns were typical of the populations for each cell type.

To quantitatively compare input strength across layers for each cell, we calculated the proportion of the excitatory input [estimated evoked input (EEI) (*22*)] to each cell from each layer by expressing the average value from each layer as a percentage of the sum from all four layers, 4Cα, 4Cβ, 5, and 6. These values are shown for all cells in our sample in Table 1. We also calculated the

Systems Neurobiology Laboratories, Salk Institute for Biological Studies, 10010 North Torrey Pines Road, La Jolla, CA 92037, USA.

*Present address: Department of Neurobiology, Harvard Medical School, 220 Longwood Avenue WAB227, Boston, MA 02115, USA.
†To whom correspondence should be addressed. E-mail: callaway@salk.edu